HHS Public Access

Author manuscript

J Immunol. Author manuscript; available in PMC 2017 April 01.

Published in final edited form as:

J Immunol. 2016 April 1; 196(7): 3088–3096. doi:10.4049/jimmunol.1501790.

Macrophage galactose-type lectin-1 (MGL1) deficiency is associated with increased neutrophilia and hyper inflammation in Gram-Negative pneumonia

Christopher N. Jondle, **Atul Sharma**, **Tanner J. Simonson**, **Benjamin Larson**, **Bibhuti B. Mishra**, and **Jyotika Sharma**[*]

Department of Basic Biomedical Sciences, The University of North Dakota School of Medicine and Health Sciences, 501 N Columbia Road, Grand Forks, North Dakota-58202-9037

Abstract

C-type lectin receptors (CLRs), the carbohydrate recognizing molecules, orchestrate host immune response in homeostasis and in inflammation. In the present study we examined the function of macrophage galactose-type lectin-1 (MGL1), a mammalian CLR, in pneumonic sepsis, a deadly immune disorder frequently associated with a non-resolving hyperinflammation. In a murine model of pneumonic sepsis using pulmonary infection with *Klebsiella pneumoniae* (KPn), the expression of MGL1 was upregulated in the lungs of KPn infected mice and the deficiency of this CLR in MGL1$^{-/-}$ mice resulted in significantly increased mortality to infection than the MGL1-sufficient wild-type mice, despite a similar bacterial burden. The phagocytic cells from MGL1$^{-/-}$ mice did not exhibit any defects in bacterial uptake and intracellular killing and were fully competent in neutrophil extracellular trap formation, a recently identified extracellular killing modality of neutrophils. Instead, the increased susceptibility of MGL1$^{-/-}$ mice seemed to correlate with severe lung pathology, indicating that MGL1 is required for resolution of pulmonary inflammation. Indeed, the MGL1$^{-/-}$ mice exhibited a hyperinflammatory response, massive pulmonary neutrophilia and increase in neutrophil-associated immune mediators. Concomitantly, MGL1 deficient neutrophils exhibited an increased influx in pneumonic lungs of KPn infected mice. Together these results show a previously undetermined role of MGL1 in controlling neutrophilia during pneumonic infection thus playing an important role in resolution of inflammation. This is the first report depicting a protective function of MGL1 in an acute pneumonic bacterial infection.

Introduction

Pattern recognition receptors (PRRs) activate innate immune responses upon detection of conserved pathogen motifs as well as self-molecules released during a pathological insult. Among the PRRs, the Toll-like receptor (TLR) family is the most characterized group of receptors known to be involved in activation and maturation of innate immune cells such as dendritic cells and macrophages, among others (1). Another family of PRRs consists of

[*]Send correspondence and reprint requests to: Jyotika Sharma, Ph.D., Department of Basic Sciences, The University of North Dakota School of Medicine and Health Sciences, 501 N Columbia Road, Grand Forks, North Dakota-58202-9037; Tel: (701) 777-2624; Fax: (701) 777-2054; jyotika.sharma@med.und.edu.

transmembrane and soluble C-type lectin receptors (CLRs), which have selective affinity for self and non-self glycan motifs in a Ca^{2+}-dependent manner (2). Due to their abundant expression on sentinel cells of innate immune system that contribute to inflammation and maintenance of immune homeostasis, CLRs act as key sensors of tissue integrity and pathological insult and play a central role in orchestrating immune responses (3).

Macrophage galactose-type C lectin 1 (MGL1) is a type 2 transmembrane CLR expressed on macrophages and immature dendritic cells with a binding specificity for galactose and/or its monosaccharide derivative, that are abundantly expressed on tumor antigen MUC1 as well as self-antigens such as gangliosides (4). Not surprisingly, MGL1 is included in the family of scavenger receptors along with macrophage mannose receptor (5) that plays a role in recognition of tumor antigens and apoptotic cells (6, 7). Although this CLR can bind antigens from *Neisseria gonorrhoeae* (8), *Campylobacter jejuni* (9) and *Bordetella pertussis* (10), its role in overall disease pathogenesis is unknown. An anti-inflammatory function of this CLR in colitis via its interaction with commensal bacteria has been reported (11). However, the current knowledge of MGL1 function in infectious diseases, particularly the pathogenesis of pneumonia and sepsis is virtually non-existent.

Sepsis is a deadly disorder characterized by a systemic hyperinflammation resulting usually from an infectious insult. An estimated 20–50% of the 750,000 sepsis and severe sepsis patients die in the US owing to the lack of effective treatment strategies (12). Infections of the lung and the respiratory tract are the main causes of severe sepsis, and 41% of these infections are due to Gram-negative bacteria (13–15). Nosocomial infections with *Klebsiella pneumoniae* (KPn) account for 5–20% of Gram-negative sepsis cases (13, 15). KPn-induced lung infection is a clinically relevant animal model of sepsis and a better understanding of this model may help to increase the knowledge about sepsis pathophysiology (16). Additionally, emergence of multidrug resistant isolates of KPn in clinical settings is a serious health concern. In this scenario an understanding of the functioning of host innate immune components that influence the outcome of KPn pneumonia might provide targets for modulation of host immune system in a beneficial manner.

In this study we examined if MGL1 plays a role in orchestrating host defense against KPn pneumosepsis. Indeed, our results suggest that MGL1-mediated responses are required for the resolution of pneumonia and an increased susceptibility of $MGL1^{-/-}$ mice correlates with the increased inflammatory response and with massive accumulation of neutrophils in the lungs of infected mice, despite similar bacterial burden. These results identify for the first time, a protective role of MGL1 in regulation of neutrophil influx and inflammatory response against pneumonic KPn sepsis.

Materials AND Methods

Bacterial strains and Mice

The KPn (ATCC strain 43816) were grown to log phase in LB medium at 37°C. All *in-vivo* experiments were performed using 6–8 weeks old female wild-type C57BL/6 (WT) or $MGL1^{-/-}$ mice on same background obtained from JAX mice (Jackson Laboratory), and

bred in the animal facility of the University of North Dakota. The animals were used according to institutional and federal guidelines.

Infection of Mice, survival and bacterial burden

Mice were anaesthetized with a mixture of 30mg/ml ketamine and 4 mg/ml xylazine in PBS and were infected intranasally with 3.0 x 10^4 CFUs in 20ul of saline, of KPn or with 20 μl of saline alone. Survival of the mice was recorded for up to 2 weeks post-infection (p.i.). Death was recorded as infection induced mortality. Mice displaying severe signs of distress (labored breathing, non-responsiveness to cage tapping, failure of grooming and feeding) were humanely sacrificed and also recorded as infection induced mortality. In some experiments, the mice were euthanized at indicated times p.i. and blood, lungs and liver were aseptically homogenized in cold PBS with Complete™ protease inhibitor cocktail (Roche Diagnostics, Germany). For the bacterial burden analyses, serially diluted homogenates and blood were plated on LB agar and incubated at 37°C overnight.

Quantitative real-time PCR

Total RNA from lungs of infected and mock control mice harvested at various times p.i. was extracted using Trizol reagent (Invitrogen) according to the manufacturers' instructions. Real-time PCR analysis was performed using SYBR green (Applied Biosystems, CA, USA) to measure the MGL1-specific mRNA by using specific primers (sense) 5′-5′-TCTCTGAAAGTGGATGTGGAGG-3′ and (anti-sense) 5′-CACTACCCAGCTCAAACACAATCC-3′ as described by us (17). The target gene expression levels were normalized to levels of the house keeping 18S gene in the same sample. Expression of MGL1 in infected samples was determined as fold change over that in control samples as calculated by using the formula $2^{-(\Delta\Delta Ct)}$.

Multi-analyte profile analysis

The lung homogenates were prepared as described for the bacterial burden analysis above and were centrifuged at 2000 x g for 15 min to clear cellular debris. The supernatants were immediately frozen at −80° C. The biomarker levels in lung homogenates were determined commercially by Myriad Rules-based Medicine (Austin, TX, USA) utilizing a multiplexed analysis.

Histological and Immunofluorescence analysis

For histological analysis, frozen lung tissues were processed as previously described (18, 19). Serial horizontal sections (10 μm thick) of frozen lung tissues thus obtained were stained with hematoxylin and eosin for pathological analysis as previously described (20, 21). For Immunofluorescence staining, the frozen lung tissue sections were stained for the detection of MGL1, using an affinity purified anti-mMGL1/CD301 goat IgG (R&D Systems, Minneapolis, MN) and visualized with Alexa Fluor® 546 donkey anti-goat IgG (Life Technologies, Grand Island, NY). The images were acquired using a Nikon eclipse 80i upright microscope (Nikon Corporation, Tokyo, Japan) with an attached cooled RTke Spot 7.3 three spot color camera (Diagnostic Instruments Inc., Sterling Heights, MI). The images

were processed and analyzed using Adobe Photoshop 7.0 software (Adobe, Mountain View, CA).

Flow Cytometry

Lungs cells were harvested from mice at 3 days p.i. and processed as previously described by us (18, 19, 22). Cells types in the lungs were quantified by staining with Pacific Blue™ anti-mouse CD11b (Clone M1/70), APC-Cy7 anti-mouse CD11c (Clone N418), FITC anti-mouse CD19 (Clone 6D5), Brilliant Violet 570 anti-mouse CD3 (Clone 17A2), APC anti-mouse Ly6G (Clone 1A8), PerCP/Cyc5.5 anti-mouse Ly6C (Clone HK1.4), PE-Cy7 anti-mouse F4-80 (Clone BM8) antibodies (Biolegend, San Diego, CA), and PE anti-mouse TCR β (Clone H57-597) antibody (Becton Dickinson Pharmingen, San Jose, CA). Enumeration of neutrophils by flow cytometry (using a BD LSR II, Becton Dickinson, San Jose, CA) was done by quantitating Ly6G+CD11b+ cells stained with Pacific Blue™ anti-mouse CD11b (Clone M1/70) and APC anti-mouse Ly6G (Clone 1A8) antibodies (Biolegend, San Diego, CA). FlowJo (Tree Star) software was used to analyze all data.

Bacterial phagocytosis and killing by neutrophils and macrophages

Bacterial phagocytosis of WT and MGL1$^{-/-}$ neutrophils and macrophages was assessed by plating on LB media, incubating at 37°C overnight, and counting colonies. For this peritoneal neutrophils from C57BL/6 and MGL1$^{-/-}$ mice were isolated using an established method of thioglycollate-induced peritonitis. Sterile 4% thioglycollate was injected in peritoneal cavity of mice and neutrophils enriched 16–18h following the injection were isolated. Five x10^5 Neutrophils were incubated with KPn (MOI 50) for 1 hour to determine bacteria uptake and 3 hours to determine bacteria killing. After 1h the neutrophils were washed two times with warm PBS and one time with RPMI before adding 2μg/mL gentamicin in RPMI (Gibco) with 10% FBS for the remaining 2h (for the 3h samples) and for 15 minute for the 1h samples. The cells were washed extensively with warm PBS before lysing with 0.1% TritonX100. Serial dilutions of the lysates were plated on LB media overnight at 37°C before colonies were counted.

Bone marrow was isolated from wild-type and MGL1$^{-/-}$ mice and the cells were differentiated to macrophages as previously described (23). On day 6 of culture, 3x10^5 macrophages were plated in 24-well flat bottom plates and were infected with KPn (MOI 50) for 1 hour to determine bacteria uptake and 3 hours to determine bacteria killing as described above.

Neutrophil Extracellular Traps

For detection of neutrophil NETs *in-vivo*, the bronchoalveolar lavage (BAL) was performed in WT and MGL1$^{-/-}$ mice at 3dp.i. (24). The lavage cells were cytocentrifuged on glass slides and were stained with Sytox Green (Molecular Probe, Eugene, OR) to visualize NETs. The percent NET formation was quantitated by dividing the number of NET-forming neutrophils by total number of cells in 8–10 random microscopic fields and multiplying the values by 100. The experiment was repeated 3 times.

Neutrophil Adoptive Transfer

Adoptive transfer of bone marrow neutrophils was performed by methods previously described with modifications (25–27). Briefly, bone marrow neutrophils were isolated from WT and MGL1$^{-/-}$ mice by gradient separation. Purified neutrophils (~80% purity determined by flow cytometry) were labeled with CellTracker Orange CMTMR (Life technologies) or CellTracker Green CMFDA (Life technologies) at 37°C for 10 minutes. Labeled cells were mixed in 1:1 ratio using 2x10^6 each group and then injected intravenously via tail vein into WT and MGL1$^{-/-}$ mice that had been infected with 3.0 x 10^4 CFUs of KPn intranasally 24h prior. Lungs were harvested 2h after the tail vein injections and processed for flow cytometry as described above. Adoptively transferred neutrophils recruited to the lungs were enumerated using LSR II flow cytometer and analyzed using FlowJo software (BD Biosciences, San Jose, CA). Relative recruitment of WT and MGL1$^{-/-}$ neutrophils was calculated as the ratio of indicated populations.

Statistical Analysis

Statistical analysis of survival studies was performed by Kaplan Meir log-rank test; bacterial burdens by non-parametric Mann-Whitney Test. All other statistical analyses were performed using the Student t test (SIGMA PLOT 8.0, Systat Software, San Jose, CA).

Results

MGL1 expression in mouse lungs during pneumonic KPn infection

To examine the role of MGL1 in KPn induced pneumonic sepsis, we first determined its transcript-level expression by real-time quantitative PCR using RNA from lungs of KPn-infected wild-type (WT) mice. The results showed that MGL1 mRNA was maximally transcribed by 3dp.i. (Fig. 1A), a time when infiltration of immune cells is peaked during infection (21, 24). To examine the expression of MGL1 at the protein level, in-situ IF microscopy was performed on lung crysections of mock control and KPn infected WT mice at indicated post-infection times. In uninfected mock controls, the expression of MGL1 was at low basal level (Fig. 1B). Upon infection, this CLR was found to be abundantly expressed at 3dp.i., consistent with the high transcript level in lungs at that time (Fig. 1B). Interestingly, in addition to some infiltrating immune cells, MGL1 appeared to be expressed prominently by endothelial and alveolar epithelial cells in the lungs of these mice. This infection induced upregulation in the expression of MGL1 in pneumonic lungs during KPn infection indicated that this CLR likely plays a role in the pathogenesis of KPn pneumonia.

Increased susceptibility of MGL1$^{-/-}$ mice to KPn pneumonia

To examine the role of MGL1 in disease development, overall disease severity and survival was compared in wild-type (WT) and MGL1$^{-/-}$ mice infected with KPn. As the WT mice are also susceptible to KPn infection, in order to dissect the role of MGL1, we experimentally standardized a sublethal dose of KPn at which 60–70% of the WT mice resolve the infection and display only transient signs of disease (ruffled fur, lethargy) early during infection. We found that MGL1$^{-/-}$ mice were significantly more susceptible to this dose and majority of mice succumbed to infection by day 5p.i. (Fig. 2A). These mice

exhibited progressive development of disease and overt signs of infection (weight loss, piloerection, hunched gait, lethargy, increased respiratory rate). The increased susceptibility of MGL1$^{-/-}$ mice clearly indicated a protective role played by this CLR during pneumonic KPn infection. To examine the impact of MGL1 deficiency on the host antibacterial defense mechanism, comparison of local and systemic bacterial burden in the organs of infected WT and MGL1−/− mice was performed. Intriguingly, there were no statistically significant differences in the bacterial loads in lungs, liver or in blood of WT and MGL1−/− mice, although the MGL1$^{-/-}$ mice tended to exhibit higher burdens at later times post-infection (Fig. 2B). Based on this data, the protective function of MGL1 did not appear to correlate with reduced bacterial burden or systemic dissemination.

Role of MGL1 in phagocyte function

We next examined the direct effect of MGL1 deficiency on the bacterial uptake and killing capability of phagocytic cells i.e. neutrophils and macrophages. As shown in Fig. 3A and B, WT and MGL1$^{-/-}$ neutrophils and macrophages were equally competent in phagocytosis and clearance of KPn. Studies from our and other laboratories have shown that KPn infection induces Neutrophil Extracellular Trap (NET) formation in-vivo in lungs of mice and that NETs can effectively inhibit the growth of KPn (24, 28). We thus compared the extent of NET formation *in-vivo* in the lungs of KPn infected WT and MGL1$^{-/-}$ mice. As shown in Fig. 3C, neutrophils isolated from BAL of infected MGL1$^{-/-}$ mice did not exhibit any defect in extracellular trap formation. Together with our observation of similar bacterial burden in WT and MGL1$^{-/-}$ mice *in-vivo*, these data indicated that protective function of MGL1 was likely independent of the bacterial clearance mechanisms during pneumonic KPn infection.

MGL1$^{-/-}$ mice exhibit severe lung pathology and hyperinflammatory response

We next compared the gross immunopathological changes and immune cell infiltration in KPn infected WT and MGL1$^{-/-}$ mice. The mock control mice of both strains displayed similar normal lung tissue morphology in H&E stained cryosections (Fig. 4i, 4v). A moderate transient infiltration of immune cells was observed in infected WT mice by day 3p.i. which was reduced substantially by 5dp.i. (Fig. 4ii–iv). The overall architecture of the lungs was largely preserved in the WT animals throughout the course of infection. In MGL1$^{-/-}$ mice on the other hand, an increased immune cell infiltration was evident even at 1dp.i. which progressively increased and resulted in pulmonary inflammation characterized by highly confluent immune cell infiltrates (Fig. 4vi–viii). To further examine the impact of MGL1 deficiency on inflammatory response, levels of multiple inflammatory cytokines in lung homogenates were compared between KPn infected WT and MGL1$^{-/-}$ mice. While the mock controls displayed low basal levels of these cytokines, KPn infected WT mice exhibited increased amounts at 3dp.i., a time of peak bacterial burden and cellular infiltration (Fig. 4B). Infected MGL1$^{-/-}$ mice on the other hand, exhibited significantly higher levels of inflammatory cytokines at that time compared to the WT mice (Fig. 4B). The levels of IL-10, an anti-inflammatory cytokine were also significantly higher in MGL1$^{-/-}$ mice, suggesting a condition of “cytokine storm” typical of sepsis, where anti-inflammatory host mediators are upregulated in an attempt to counter-balance the systemic inflammatory response (29–31). Together, our results show that MGL1 deficiency did not

render the mice defective in their ability to mount an anti-inflammatory response to counter the on-going inflammation; instead these mice displayed a hyperinflammatory phenotype typically associated with sepsis. Our observations thus raised the possibility that despite a similar bacterial burden, increased lung pathology and hyperinflammatory response is causing increased susceptibility of MGL1$^{-/-}$ mice to KPn infection.

MGL1$^{-/-}$ mice display altered neutrophil accumulation and neutrophilic immune mediators

Pneumonic infection with KPn typically results in immune cell infiltration in lungs. To examine if there were differences in the immune cell types infiltrating in the lungs of WT versus MGL1$^{-/-}$ mice, flow cytometry analysis of total lung cells was performed. The results revealed that the percent as well as absolute numbers of Ly6G+; Ly6C+ and CD11b+ myeloid cells were significantly higher in the infected MGL1$^{-/-}$ lungs than those in the WT mice (Fig. 5A and B). We found no significant differences in the numbers of macrophages (F4/80+), dendritic cells (CD11c+), αβ T cells (TCRβ+) or B cells (CD19+). Further analysis of the data revealed that the percent as well as total numbers of Ly6G+CD11b+ neutrophils were increased 2–3 fold in the lungs of MGL1$^{-/-}$ mice upon infection, as compared to the WT mice (Fig. 5C). This indicated that MGL1 likely plays a role in regulating neutrophil infiltration and that increased susceptibility of these mice may be due to excessive neutrophil accumulation contributing to exacerbated lung pathology. This was further corroborated with the analysis of neutrophil associated immune mediators which revealed significantly higher levels of neutrophil chemoattractants (CXCL1, CXCL6), neutrophil survival mediator (GM-CSF) and neutrophil activation markers (MMP9, MPO) in lung homogenates of MGL1$^{-/-}$ mice, as compared to their WT counterparts (Fig. 6). Together our data suggested a neutrophilia-promoting effect of MGL1 deficiency in KPn pneumosepsis, which results in severe pathology and hyperinflammatory response contributing to the increased susceptibility of MGL1$^{-/-}$ mice to KPn pneumonia.

MGL-1 deficiency causes increased neutrophil influx into the lungs during KPn pneumonia

In order to gain mechanistic insights into the role of MGL1 in neutrophil accumulation, we performed neutrophil adoptive transfer using WT and MGL1$^{-/-}$ neutrophils labelled with two different intracellular dyes. Injecting a mix of the two types of neutrophils and calculating the ratio of MGL1$^{-/-}$ neutrophils to WT neutrophils and vice versa, allowed us to assess the relative migration efficiency of WT and MGL1−/− neutrophils in the exact same microenvironment (Fig. 7A). Consistent with our pathological and flow cytometry findings, we observed that MGL1$^{-/-}$ neutrophils were recruited at a higher rate than their WT counterparts in pneumonic lungs of recipient WT as well as MGL1$^{-/-}$ mice (Fig.7B). Deficiency of MGL1 on endothelial and possibly other resident cells did not appear to affect neutrophil recruitment, as evidenced by similar migration of WT neutrophils in MGL1$^{-/-}$ and WT mice (Fig. 7B black bar). These results further solidified the fact that MGL1$^{-/-}$ neutrophils exhibit an increased capacity to infiltrate the lungs during KPn pneumonia indicating a previously undetermined role of MGL1 in controlling neutrophilia during pneumonic infection.

Discussion

Gram-negative pneumonic sepsis remains a serious healthcare challenge despite effective antibiotic treatments. This underscores that erratic host response to the infectious insult is an important element in determining the outcome of the disease. Here we report that MGL1, a host CLR, impacts the outcome of Klebsiella induced pneumosepsis as evidenced by a reduced survival, severe neutrophilic lung pathology and hyperinflammation of MGL1$^{-/-}$ mice. While the antimicrobial functions of neutrophils and macrophages remain unaffected by MGL1 deficiency, the mechanistic basis for the observed differences between the WT and MGL1$^{-/-}$ mice appeared to be de-regulated neutrophil influx and excessive, non-resolving inflammation. Our study shows, for the first time, a protective role of MGL1 in Gram-negative pneumonic sepsis in part by controlling neutrophil influx into the lungs.

CLRs, by way of their abundant expression on phagocytic cells, can mediate pathogen uptake and antigen presentation (32–34). MGL1 has been shown to mediate the attachment and entry of influenza A virus (35) and recombinant MGL1 can bind intestinal commensal bacteria (11). We examined if this CLR plays any role in KPn uptake and clearance by phagocytic cells which may explain the increased susceptibility of MGL1$^{-/-}$ mice to this infection. Strikingly, we observed no difference in the phagocytic and bacterial killing capacity of neutrophils and macrophages, two cells types involved in KPn phagocytosis and clearance. Neutrophils can also kill pathogens by the release of NETs composed of chromatin decorated with neutrophil derived proteins (36). The NETs have been demonstrated to play a role in controlling KPn growth (24, 28, 37). However, similar to the phagocytosis and intracellular killing, we did not find any defect in NETs formation in MGL1$^{-/-}$ neutrophils in-vivo. Together, these observations correlated with similar local and systemic bacterial burden in WT and MGL-1$^{-/-}$ mice and led to the possibility that the poor disease outcome in the absence of MGL1 is due to its impact on host immune responses other than those directly affecting antibacterial mechanisms.

Unlike humans, who express only one form of MGL, mice have two orthologues of this CLR: MGL1 and MGL2 (4). MGL1 and MGL2 have been suggested to perform non-redundant functions with MGL1 being most widely studied for its role in inflammatory and infectious disease conditions (4). To the best of our knowledge, there are no reports to suggest that MGL2 expression is modulated due to a deficiency of MGL1 in MGL1$^{-/-}$ mice. While this will require detailed structural and functional studies utilizing MGL2$^{-/-}$ mice, our data presented in this manuscript shows a clear phenotype of increased susceptibility and poor disease outcome in the absence of MGL1 in MGL1$^{-/-}$ mice. Moreover, unlike MGL1, KPn infection did not cause any increase in expression of MGL2 at the transcript level in infected mouse lungs as compared to the uninfected control mice (data not shown). Whether or not MGL2 is involved synergistically, directly or indirectly; could be a topic of future investigation.

Despite a similar bacterial burden, MGL1 deficiency resulted in more severe lung pathology and heightened inflammatory response. These mice displayed hyperinflammation and a lack of resolution in their lungs, suggesting a protective, pro-resolving role of MGL1 in pneumosepsis. Both anti-as well as pro-inflammatory functions of MGL1 have been

described in distinct pathological conditions. Increased susceptibility of MGL1$^{-/-}$ mice to helminth parasitic infection with *Taenia crassiceps* was shown to correlate with reduction in the levels of proinflammtory cytokines (38). An MGL-dependent induction of pro-inflammatory cytokines, TNF-α, IL-6 and IFN-γ in *Bordetella pertussis* stimulated mast cells was reported (10), however, the relevance of these findings to overall disease outcome was not examined. In contrast to these studies, an anti-inflammatory role of MGL1 was described in experimental colitis, where the protective function of MGL1 was attributed to induction of IL-10 by colonic lamina propria macrophages in response to commensal bacteria (11). We observed an excessive upregulation of both pro- as well as anti-inflammatory cytokines in MGL1$^{-/-}$ mice undergoing KPn pneumoseptic infection. It is likely that the presence of multiple PAMPs and alarmins released due to bacterial growth and/or inflammation contributes to the effect of MGL1 deficiency and causes stimulation of multiple PRRs on immune cells resulting in a mixed pro-and anti-inflammatory hyper response reminiscent of characteristic cytokine storm. Indeed, a cross-talk between CLRs and Toll-like receptors (TLR)-induced immune responses has been reported where CLR mediated uptake of Schistosoma antigens suppresses TLR-mediated dendritic cell maturation (39). Whether an inverse relationship between MGL1 and TLR signaling exists or if MGL1 negatively regulates TLR stimulation in KPn pneumonia remains to be determined. Nonetheless, the fact that a hypeinflammation and more severe pathological changes were observed in MGL1$^{-/-}$ mice despite a similar bacterial burden indicate that MGL1 negatively regulates the inflammation and a perpetuation of inflammation rather than the bacterial growth contributes to lethality of MGL1−/− mice.

We found that KPn infected MGL1$^{-/-}$ mice exhibited significantly increased neutrophil accumulation in their lungs. Neutrophil mediated responses are essential for combating pneumonic bacterial infection and their protective role in sepsis and KPn infection in particular has been described elegantly (40, 41). However, persistent accumulation of neutrophils can lead to bystander tissue destruction, owing to their tissue destructive cargo. Accumulation of large numbers of neutrophils in the lungs of MGL1$^{-/-}$ mice and higher amounts of their associated inflammatory mediators suggested that there is a defect in neutrophil turnover in these mice. This could either be due to increased influx of neutrophils into the lungs; due to a defect in their clearance by efferocytosis; or a combination of both. While we are currently investigating the role of MGL1 in efferocytosis, our adoptive transfer experiment showed that MGL1 deficiency on neutrophils significantly increases their capacity to infiltrate the lungs of pneumonic mice. This suggested a novel role of MGL1 as a negative regulator of neutrophil influx, although previous studies have implicated this CLR in trafficking of other myeloid cell types. Relevant to our study, mouse MGL has been reported to impede migration of immature dendritic cells (DCs) via its interaction with its glycan ligands on endothelium, and blockage of MGL results in an enhanced random mobility of these cells (42). Mature DCs lose MGL expression (43), thus enabling these cells to overcome the negative effect of MGL and egress. Similar mechanisms could be at play in our model where MGL1 negatively regulates epithelium-neutrophil interactions thereby impeding neutrophil infiltration into the intrapulmonary space and retaining them into circulation, and only after MGL1 expression is lost, are these neutrophils able to infiltrate into the lungs. This could also explain why we could not detect MGL1 expression

on neutrophils infiltrating the lungs of KPn infected WT mice (data not shown). Curiously, while MGL1 was expressed on bronchial epithelial and endothelial cells in lungs, we did not see a significant effect of endothelial cell expressed MGL1 on neutrophil influx (evidenced by similar infiltration of labelled WT neutrophils in $MGL1^{-/-}$ and WT mice). While the role of MGL1 expressed on other resident cells cannot be ruled out at this time, the significance of this endothelial expression pattern remains to be experimentally determined.

In the absence of MGL1 we also observed significantly higher induction of neutrophil chemoattractants (CXCL1 and CXCL6), neutrophil survival mediator (GM-CSF) and neutrophil activation markers (MMP9, MPO) in $MGL1^{-/-}$ mice, as compared to their WT counterparts. These results further support the notion that MGL1 is likely involved in neutrophil turnover and the absence of MGL1 results in greater and prolonged accumulation of neutrophils in lungs of mice. This leads to a greater neutrophil-mediated inflammation and lung pathology observed in $MGL1^{-/-}$ mice as compared to their WT counterparts where the neutrophils infiltrate transiently and are cleared off as the infection resolves. These observations clearly suggest that while deficiency of MGL1 does not impair bacterial phagocytosis and activation of neutrophils, this CLR is required for regulating neutrophil trafficking.

In summary, this study shows that MGL1 plays an important role in mitigating the inflammation during a pneumonic infection, by negatively regulating the neutrophil influx. This study opens up new avenues of research on the role of MGL1 in neutrophil trafficking. This can have major implications in the therapeutic measurements of inflammation associated disorders.

Acknowledgments

This work was supported by National Institutes of Health, National Institute of Allergy and Infectious Diseases Grants R21, R01 and Faculty Start-up funds (to JS).

The authors thank Dr. Anthony Steichen for technical help with flow cytometry and Dr. Sisi He with tail vein injections. We also thank the Flow Cytometry and imaging core facilities at the UND for providing the instrumentation and technical support for the flow cytometry and imaging data presented here.

References

1. Kumagai Y, Takeuchi O, Akira S. Pathogen recognition by innate receptors. Journal of infection and chemotherapy : official journal of the Japan Society of Chemotherapy. 2008; 14:86–92. [PubMed: 18622669]
2. Rabinovich GA, van Kooyk Y, Cobb BA. Glycobiology of immune responses. Annals of the New York Academy of Sciences. 2012; 1253:1–15. [PubMed: 22524422]
3. Dambuza IM, Brown GD. C-type lectins in immunity: recent developments. Current opinion in immunology. 2015; 32:21–27. [PubMed: 25553393]
4. van Kooyk Y, Ilarregui JM, van Vliet SJ. Novel insights into the immunomodulatory role of the dendritic cell and macrophage-expressed C-type lectin MGL. Immunobiology. 2015; 220:185–192. [PubMed: 25454488]
5. van Vliet SJ, Saeland E, van Kooyk Y. Sweet preferences of MGL: carbohydrate specificity and function. Trends in immunology. 2008; 29:83–90. [PubMed: 18249034]
6. van Vliet SJ, van Liempt E, Saeland E, Aarnoudse CA, Appelmelk B, Irimura T, Geijtenbeek TB, Blixt O, Alvarez R, van Die I, van Kooyk Y. Carbohydrate profiling reveals a distinctive role for the

C-type lectin MGL in the recognition of helminth parasites and tumor antigens by dendritic cells. International immunology. 2005; 17:661–669. [PubMed: 15802303]

7. Yuita H, Tsuiji M, Tajika Y, Matsumoto Y, Hirano K, Suzuki N, Irimura T. Retardation of removal of radiation-induced apoptotic cells in developing neural tubes in macrophage galactose-type C-type lectin-1-deficient mouse embryos. Glycobiology. 2005; 15:1368–1375. [PubMed: 16096344]
8. van Vliet SJ, Steeghs L, Bruijns SC, Vaezirad MM, Snijders Blok C, Arenas Busto JA, Deken M, van Putten JP, van Kooyk Y. Variation of Neisseria gonorrhoeae lipooligosaccharide directs dendritic cell-induced T helper responses. PLoS pathogens. 2009; 5:e1000625. [PubMed: 19834553]
9. van Sorge NM, Bleumink NM, van Vliet SJ, Saeland E, van der Pol WL, van Kooyk Y, van Putten JP. N-glycosylated proteins and distinct lipooligosaccharide glycoforms of Campylobacter jejuni target the human C-type lectin receptor MGL. Cellular microbiology. 2009; 11:1768–1781. [PubMed: 19681908]
10. Vukman KV, Ravida A, Aldridge AM, O'Neill SM. Mannose receptor and macrophage galactose-type lectin are involved in Bordetella pertussis mast cell interaction. Journal of leukocyte biology. 2013; 94:439–448. [PubMed: 23794711]
11. Saba K, Denda-Nagai K, Irimura T. A C-type lectin MGL1/CD301a plays an anti-inflammatory role in murine experimental colitis. The American journal of pathology. 2009; 174:144–152. [PubMed: 19095961]
12. Angus DC, Linde-Zwirble WT, Lidicker J, Clermont G, Carcillo J, Pinsky MR. Epidemiology of severe sepsis in the United States: analysis of incidence, outcome, and associated costs of care. Critical care medicine. 2001; 29:1303–1310. [PubMed: 11445675]
13. Eddens T, Kolls JK. Host defenses against bacterial lower respiratory tract infection. Current opinion in immunology. 2012; 24:424–430. [PubMed: 22841348]
14. Kang CI, Song JH, Chung DR, Peck KR, Ko KS, Yeom JS, Ki HK, Son JS, Lee SS, Kim YS, Jung SI, Kim SW, Chang HH, Ryu SY, Kwon KT, Lee H, Moon C, Korean D. Network for Study of Infectious. Risk factors and pathogenic significance of severe sepsis and septic shock in 2286 patients with gram-negative bacteremia. The Journal of infection. 2011; 62:26–33. [PubMed: 21056057]
15. Nordmann P, Cuzon G, Naas T. The real threat of Klebsiella pneumoniae carbapenemase-producing bacteria. The Lancet infectious diseases. 2009; 9:228–236. [PubMed: 19324295]
16. Sordi R, Menezes-de-Lima O, Della-Justina AM, Rezende E, Assreuy J. Pneumonia-induced sepsis in mice: temporal study of inflammatory and cardiovascular parameters. International journal of experimental pathology. 2013; 94:144–155. [PubMed: 23441627]
17. Mishra BB, Gundra UM, Teale JM. STAT6(−)/(−) mice exhibit decreased cells with alternatively activated macrophage phenotypes and enhanced disease severity in murine neurocysticercosis. Journal of neuroimmunology. 2011; 232:26–34. [PubMed: 21051093]
18. Mares CA, Ojeda SS, Morris EG, Li Q, Teale JM. Initial delay in the immune response to Francisella tularensis is followed by hypercytokinemia characteristic of severe sepsis and correlating with upregulation and release of damage-associated molecular patterns. Infection and immunity. 2008; 76:3001–3010. [PubMed: 18411294]
19. Sharma J, Li Q, Mishra BB, Pena C, Teale JM. Lethal pulmonary infection with Francisella novicida is associated with severe sepsis. Journal of leukocyte biology. 2009; 86:491–504. [PubMed: 19401387]
20. Gundra UM, Mishra BB, Wong K, Teale JM. Increased disease severity of parasite-infected TLR2−/− mice is correlated with decreased central nervous system inflammation and reduced numbers of cells with alternatively activated macrophage phenotypes in a murine model of neurocysticercosis. Infection and immunity. 2011; 79:2586–2596. [PubMed: 21482681]
21. Steichen AL, Binstock BJ, Mishra BB, Sharma J. C-type lectin receptor Clec4d plays a protective role in resolution of Gram-negative pneumonia. Journal of leukocyte biology. 2013; 94:393–398. [PubMed: 23709686]
22. Sharma J, Li Q, Mishra BB, Georges MJ, Teale JM. Vaccination with an attenuated strain of Francisella novicida prevents T-cell depletion and protects mice infected with the wild-type strain from severe sepsis. Infection and immunity. 2009; 77:4314–4326. [PubMed: 19635830]

23. Mariathasan S, Weiss DS, Dixit VM, Monack DM. Innate immunity against Francisella tularensis is dependent on the ASC/caspase-1 axis. The Journal of experimental medicine. 2005; 202:1043–1049. [PubMed: 16230474]
24. Sharma A, Steichen AL, Jondle CN, Mishra BB, Sharma J. Protective role of mincle in bacterial pneumonia by regulation of neutrophil mediated phagocytosis and extracellular trap formation. The Journal of infectious diseases. 2014; 209:1837–1846. [PubMed: 24353272]
25. Sakai J, Li J, Subramanian KK, Mondal S, Bajrami B, Hattori H, Jia Y, Dickinson BC, Zhong J, Ye K, Chang CJ, Ho YS, Zhou J, Luo HR. Reactive oxygen species-induced actin glutathionylation controls actin dynamics in neutrophils. Immunity. 2012; 37:1037–1049. [PubMed: 23159440]
26. Swamydas M, Lionakis MS. Isolation, purification and labeling of mouse bone marrow neutrophils for functional studies and adoptive transfer experiments. Journal of visualized experiments : JoVE. 2013:e50586. [PubMed: 23892876]
27. Swamydas, M.; Luo, Y.; Dorf, ME.; Lionakis, MS. Isolation of Mouse Neutrophils. In: Coligan, John E., et al., editors. Current protocols in immunology. 2015. p. 110p. 3 20 21-23 20 15.
28. Achouiti A, Vogl T, Urban CF, Rohm M, Hommes TJ, van Zoelen MA, Florquin S, Roth J, van't Veer C, de Vos AF, van der Poll T. Myeloid-related protein-14 contributes to protective immunity in gram-negative pneumonia derived sepsis. PLoS pathogens. 2012; 8:e1002987. [PubMed: 23133376]
29. Matera G, Puccio R, Giancotti A, Quirino A, Pulicari MC, Zicca E, Caroleo S, Renzulli A, Liberto MC, Foca A. Impact of interleukin-10, soluble CD25 and interferon-gamma on the prognosis and early diagnosis of bacteremic systemic inflammatory response syndrome: a prospective observational study. Critical care. 2013; 17:R64. [PubMed: 23561467]
30. Oh SJ, Kim JH, Chung DH. NOD2-mediated suppression of CD55 on neutrophils enhances C5a generation during polymicrobial sepsis. PLoS pathogens. 2013; 9:e1003351. [PubMed: 23675299]
31. Sugitharini V, Prema A, Berla Thangam E. Inflammatory mediators of systemic inflammation in neonatal sepsis. Inflammation research : official journal of the European Histamine Research Society … [et al.]. 2013
32. Geijtenbeek TB, Gringhuis SI. Signalling through C-type lectin receptors: shaping immune responses. Nature reviews. Immunology. 2009; 9:465–479.
33. Robinson MJ, Sancho D, Slack EC, LeibundGut-Landmann S, Reis e Sousa C. Myeloid C-type lectins in innate immunity. Nature immunology. 2006; 7:1258–1265. [PubMed: 17110942]
34. van Kooyk Y. C-type lectins on dendritic cells: key modulators for the induction of immune responses. Biochemical Society transactions. 2008; 36:1478–1481. [PubMed: 19021579]
35. Ng WC, Liong S, Tate MD, Irimura T, Denda-Nagai K, Brooks AG, Londrigan SL, Reading PC. The macrophage galactose-type lectin can function as an attachment and entry receptor for influenza virus. Journal of virology. 2014; 88:1659–1672. [PubMed: 24257596]
36. Camicia G, Pozner R, de Larranaga G. Neutrophil extracellular traps in sepsis. Shock. 2014; 42:286–294. [PubMed: 25004062]
37. Brinkmann V, Reichard U, Goosmann C, Fauler B, Uhlemann Y, Weiss DS, Weinrauch Y, Zychlinsky A. Neutrophil extracellular traps kill bacteria. Science. 2004; 303:1532–1535. [PubMed: 15001782]
38. Montero-Barrera D, Valderrama-Carvajal H, Terrazas CA, Rojas-Hernandez S, Ledesma-Soto Y, Vera-Arias L, Carrasco-Yepez M, Gomez-Garcia L, Martinez-Saucedo D, Becerra-Diaz M, Terrazas LI. The macrophage galactose-type lectin-1 (MGL1) recognizes Taenia crassiceps antigens, triggers intracellular signaling, and is critical for resistance to this infection. BioMed research international. 2015; 2015:615865. [PubMed: 25664320]
39. van Liempt E, van Vliet SJ, Engering A, Garcia Vallejo JJ, Bank CM, Sanchez-Hernandez M, van Kooyk Y, van Die I. Schistosoma mansoni soluble egg antigens are internalized by human dendritic cells through multiple C-type lectins and suppress TLR-induced dendritic cell activation. Molecular immunology. 2007; 44:2605–2615. [PubMed: 17241663]
40. Batra S, Cai S, Balamayooran G, Jeyaseelan S. Intrapulmonary administration of leukotriene B(4) augments neutrophil accumulation and responses in the lung to Klebsiella infection in CXCL1 knockout mice. Journal of immunology. 2012; 188:3458–3468.

41. Kovach MA, Standiford TJ. The function of neutrophils in sepsis. Current opinion in infectious diseases. 2012; 25:321–327. [PubMed: 22421753]

42. van Vliet SJ, Paessens LC, Broks-van den Berg VC, Geijtenbeek TB, van Kooyk Y. The C-type lectin macrophage galactose-type lectin impedes migration of immature APCs. Journal of immunology. 2008; 181:3148–3155.

43. van Vliet SJ, Gringhuis SI, Geijtenbeek TB, van Kooyk Y. Regulation of effector T cells by antigen-presenting cells via interaction of the C-type lectin MGL with CD45. Nature immunology. 2006; 7:1200–1208. [PubMed: 16998493]

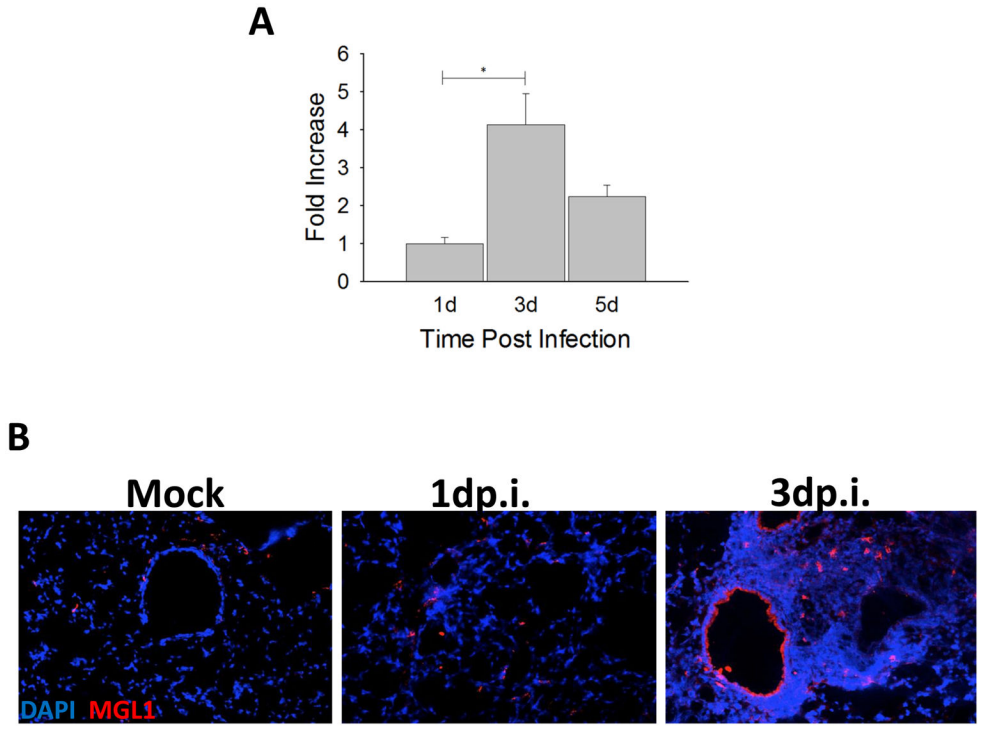

Figure 1.

MGL1 is upregulated in the lungs of *Klebsiella pneumoniae* (KPn) infected pneumonic mice. **(A)** Total RNA was extracted by Trizol method from the lungs of KPn infected wild-type (WT) C57/BL6 mice, harvested at indicated times post-infection. The mRNA levels of MGL1 were analyzed by real-time PCR as described in Methods and are expressed as fold changes over the levels in mock control mice calculated by using the formula $2^{-(\Delta\Delta Ct)}$. Data shown are the mean ± SEM of 3–4 mice per time point in two independent experiments. Significant differences were measured by Student's *t* test ($p < 0.05$) (**B)** MGL1 expression was examined by immunofluorescence staining on lung cryosections of mock control and KPn infected wild-type mice harvested at indicated times post-infection using an affinity purified anti-mouse MGL1 goat IgG followed by Alexa Fluor® 546 labelled (red) donkey anti-goat IgG. Nuclei (blue) were stained with 4′,6′-diamidino-2-phenylindole dilactate. Images shown are representative of 3 independent experiments with 3–4 mice each.

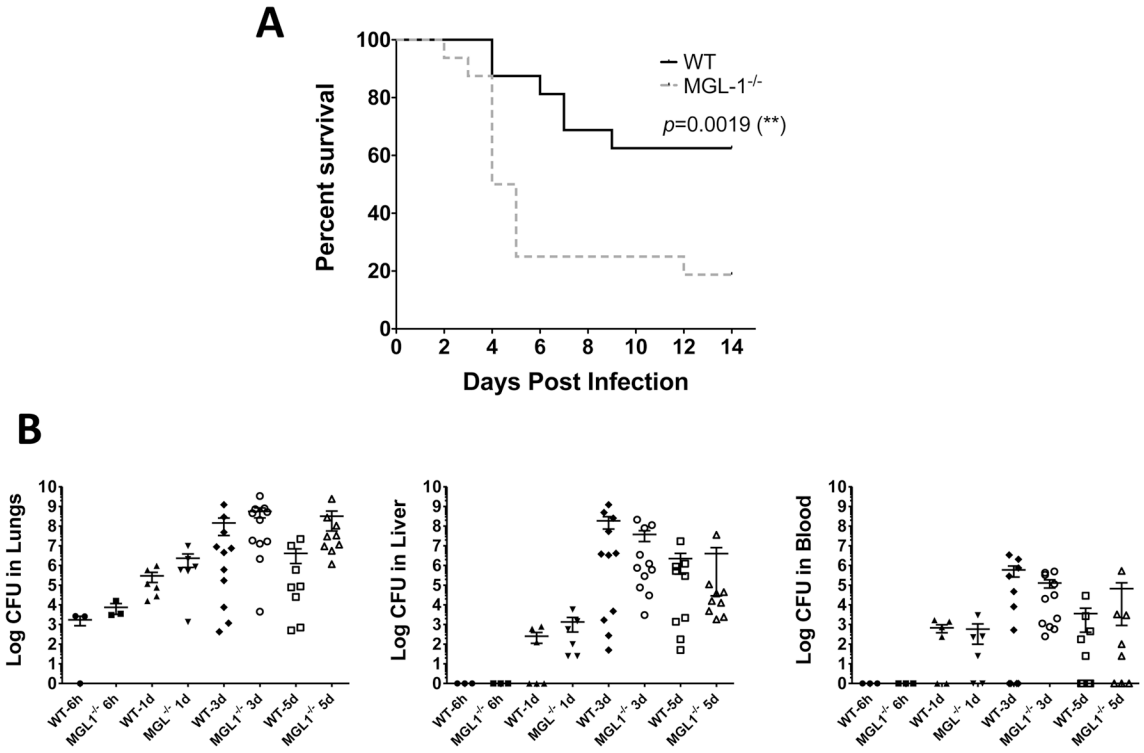

Figure 2.

MGL1$^{-/-}$ mice exhibit reduced survival despite similar bacterial burden as the WT mice. **(A)** WT and MGL1$^{-/-}$ mice were intranasally infected with 3.0x10^4 CFUs of KPn in 20μl of sterile PBS and were assessed daily for disease severity. The survival was monitored for two week. Statistical comparison of susceptibility was done by Kaplan-Meier survival curve statistical analysis (p=0.0019 **). The data shown is from 3 independent experiments (n=16). **(B)** WT and MGL1$^{-/-}$ were intranasally infected with KPn. At indicated times post infection the mice were sacrificed, systemic organs were isolated, homogenized and plated as described in Materials and Methods. Bacterial burden was enumerated after incubating the plates overnight at 37°C. No significant differences in bacterial burden (using non-parametric Mann-Whitney test) in WT and MGL1$^{-/-}$ were found. Each symbol in the scatter plots represents individual mouse and the data is from 3–4 independent experiments.

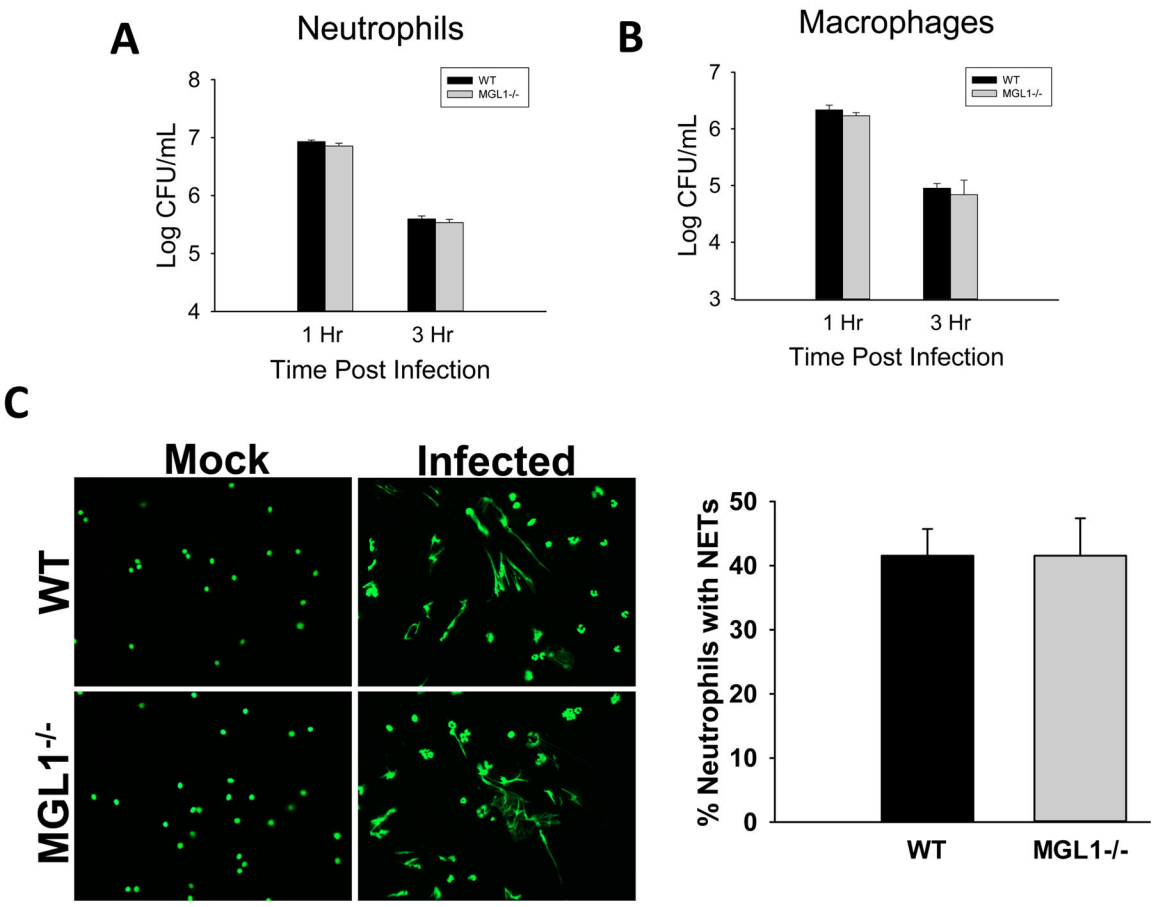

Figure 3.

MGL1 deficiency does not impair bacterial clearance by phagocytes. Bacterial uptake and killing capacity of MGL1$^{-/-}$ and WT neutrophils **(A)** or bone-marrow derived macrophages **(B)** was determined at 1h and 3h by assessing intracellular CFUs in these cells as described in Methods. Data from a representative of 3 independent experiments is shown. (**C)** Neutrophils isolated from bronchoalveolar lavage fluid (BAL) of WT (upper panel) and MGL1$^{-/-}$ (lower panel) mice infected with KPn, were cytocentrifuged and stained with Sytox Green to visualize extracellular traps (NETs). Magnification 200X. Bar graph shows quantitation of NET forming neutrophils in BAL from KPn infected WT and MGL1$^{-/-}$ mice. Data are mean ± SEM from 8 mice per group in 3 independent experiments.

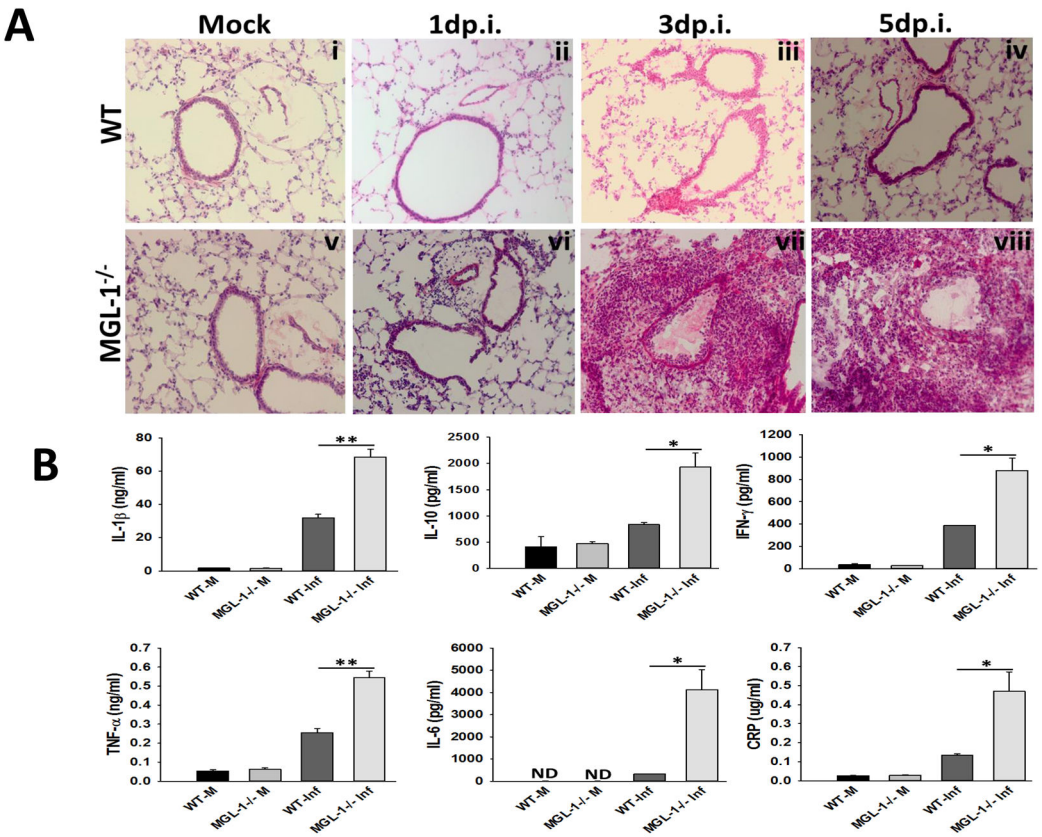

Figure 4.

Pneumonic MGL1$^{-/-}$ mice exhibit severe lung pathology and hyperinflammatory response. **(A)** Hematoxylin & Eosin staining of lung cryosections from mock control (i and v) and KPn infected WT (ii, iii, iv) and MGL1$^{-/-}$ (vi, vii, viii) mice isolated at indicated times post-infection. Magnification 200X. **(B)** The lungs from mock control (WT-M and MGL1$^{-/-}$ M) and KPn infected WT and MGL1$^{-/-}$ (WT-Inf and MGL1$^{-/-}$ Inf) mice isolated at 3d p.i. were homogenized in PBS with protease inhibitors and analyzed commercially for host immune mediators by rodent multi-analyte profile (Myriad™ Rules-Based Medicine, Austin, TX). Results shown are mean ± SEM of 3–4 each infected and mock control mice from 2–3 independent experiments. Statistical significance are denoted by asterisks (*, $p<0.05$; **, $p<0.005$). CRP; C-reactive protein.

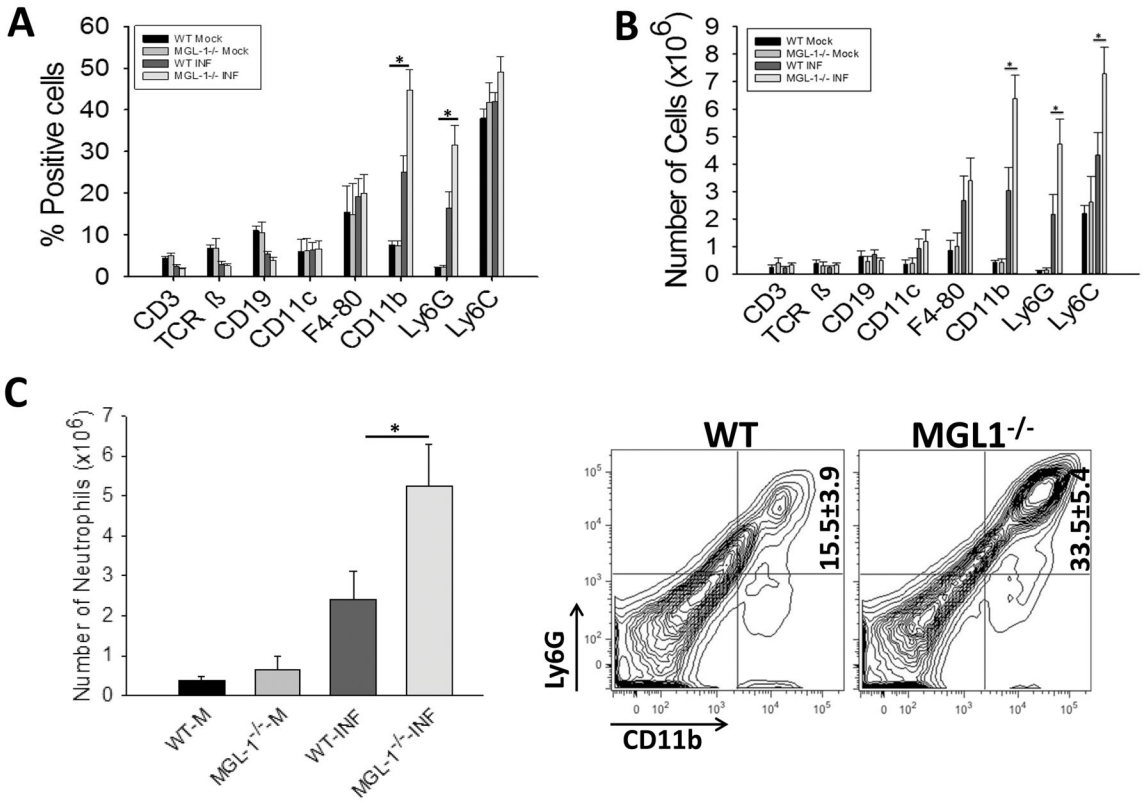

Figure 5.

Pneumonic MGL1/$^{-/-}$ mice exhibit increased neutrophil accumulation in their lungs. (**A)** Flow cytometry analysis of total lung cells from mock and KPn infected WT and MGL1$^{-/-}$ at 3dp.i. Total lungs cells were isolated from mice by collagenase treatment followed by staining with antibodies against indicated cell markers as described in methods. Each bar represents percent cells positive for individual markers in lungs of indicated experimental mice. (**B)** Shows total number of cells positive for indicated cell markers. Data shown are the mean ± SEM of 5–6 mice from 3–4 independent experiments. Statistical significance are denoted by asterisks (*, $p<0.05$). (**C)** Ly6G+CD11b+ neutrophils in lungs of KPn infected WT and MGL1$^{-/-}$ mice at 3dp.i. The cells were double-stained with anti-Ly6G-APC and anti-CD11b-Pacific Blue antibodies as markers for neutrophils. The bar graph shows mean ± SEM of total number of neutrophils in lungs of 3–4 mock control and 4–5 KPn infected WT and MGL1$^{-/-}$ mice each from 3 independent experiments. Contour plots shown on the right are from one representative experiment. Statistical significance are denoted by asterisks (*, $p<0.05$).

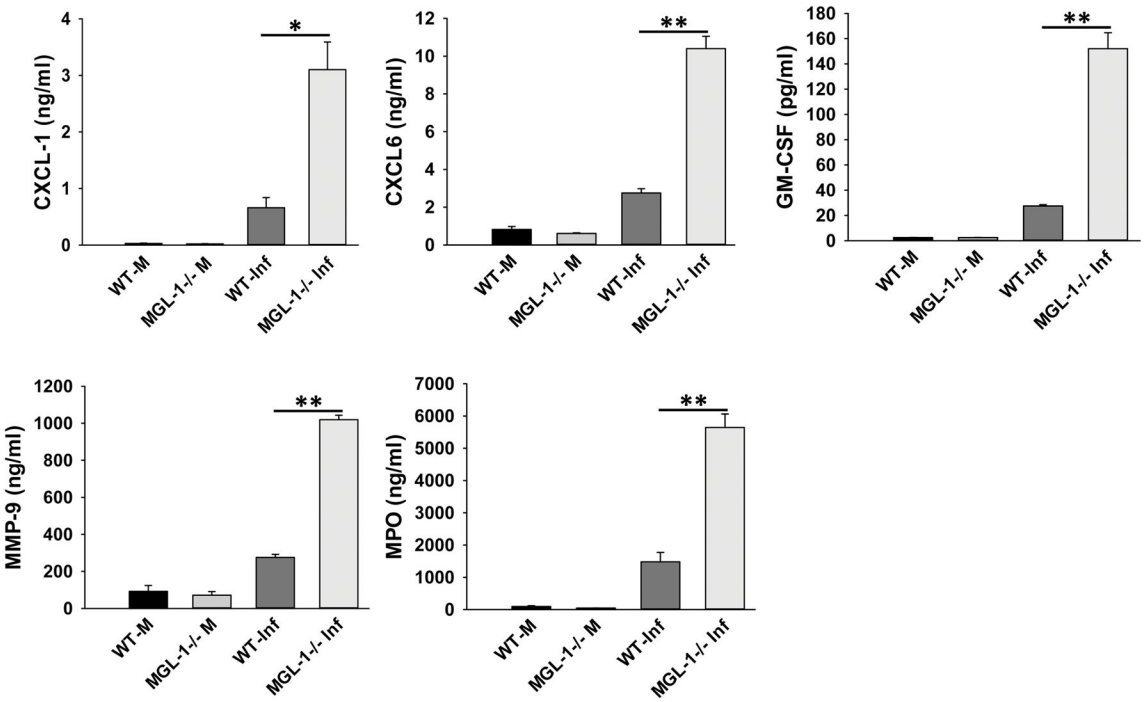

Figure 6.

Pneumonic MGL1$^{-/-}$ mice exhibit increased levels of neutrophil associated immune mediators. The lungs from mock control and KPn infected WT and MGL1$^{-/-}$ mice were harvested at 3dp.i. and analyzed commercially for host immune mediators by rodent multi-analyte profile (Myriad^{TM} Rules-Based Medicine, Austin, TX). Levels of neutrophil chemoattractants and growth factor (CXCL1, CXCL6, GM-CSF) and activation markers (matrix metalloproteinase-9, MMP-9 and myeloperoxidase, MPO) are shown. Results shown are mean ± SEM of 3–4 each infected and mock control mice from 2–3 independent experiments. Statistical significance are denoted by asterisks (*, $p<0.05$; **, $p<0.005$).

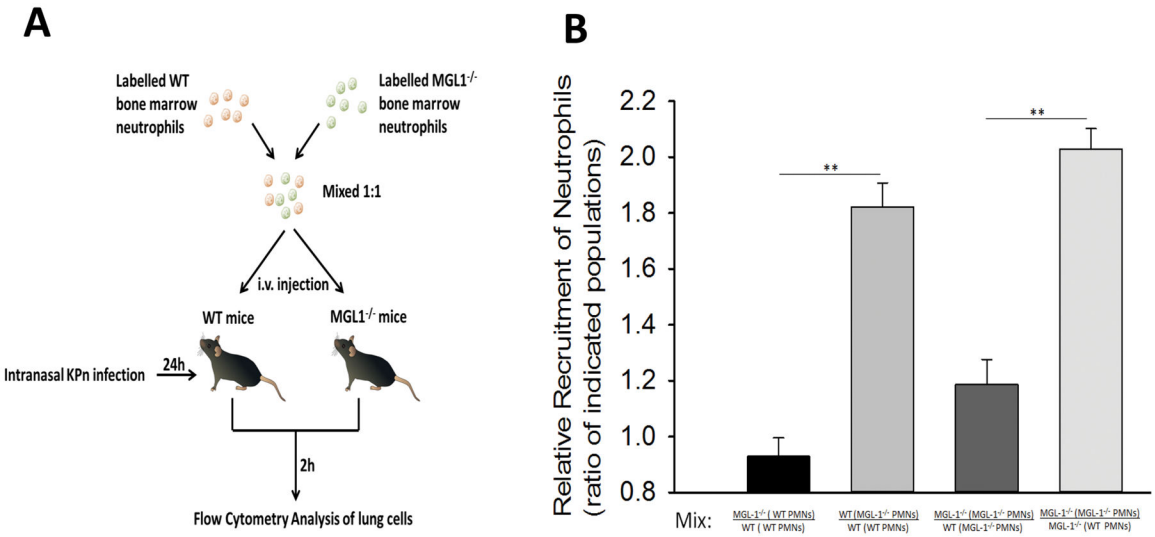

Figure 7.

MGL1 deficiency causes increased neutrophil influx in the pneumonic lungs. **(A)** Schematic representation of the adoptive transfer experiment as described in the Methods. Purified bone marrow neutrophils from WT mice were labelled with CellTracker Orange CMTMR and those from MGL1−/− mice labeled with CellTracker Green CMFDA, mixed in 1:1 ratio and injected intravenously (i.v.) into WT or $MGL1^{-/-}$ recipient mice infected intranasally with KPn 24h prior to injection. Lungs were harvested 2 hrs after the adoptive transfer and processed for flow cytometry. **(B)** Relative recruitment of MGL1−/− and WT neutrophils in each mouse strain is depicted as the ratio of indicated populations in the KPn infected lungs. Data shown are mean ± SEM form 9 mice per group in 3 independent. Statistical significance are denoted by asterisks (**, $p<0.005$).